Eur. Phys. J. D **5**, 179–184 (1999)

THE EUROPEAN PHYSICAL JOURNAL D

EDP Sciences

The shapes of Auger decay lines in photoelectron satellite spectra

V.G. Yarzhemsky[1,a] and F.P. Larkins[2]

[1] Kurnakov Institute of General and Inorganic Chemistry of Russian Academy of Sciences, 31 Leninsky, 117907, Moscow, Russia
[2] School of Chemistry, The University of Melbourne, Parkville, Victoria 3052, Australia

Received: 25 May 1998 / Accepted: 2 October 1998

Abstract. The theory of the shapes of Auger decay lines of satellite two-hole-one particle states accompanying photoionization based on the Green's function method is developed. The lineshapes of Auger decay of satellite states $[2s2p](^{1,3}P)3s(^2P)$, $[2s2p](^1P)4s(^2P)$ and $[3s3p](^3P)4s(^2P)$ in valence p-photoelectron spectra of Ne and Ar atoms are calculated (hole states are indicated by square brackets throughout). It is shown that in some cases the Auger lineshapes reproduce the shape of the photoelectron satellite line, but in other cases Auger line may be narrower then the photoelectron line and may have opposite direction of asymmetry. The theoretical results are in agreement with experimental low-energy Auger spectra.

PACS. 03.65.-w Quantum mechanics – 32.70.Jz Line shapes, widths, and shifts – 32.80.Fb Photoionization of atoms and ions

1 Introduction

Recent high-resolution photoelectron spectra of noble gases show a number of satellite lines of very different shapes [1–5]. These excited double-hole-one-particle states appear in addition to single-hole states due to electron-electron correlations. The asymmetrical broadening of satellites is a result of interference of two correlation processes: a direct excitation of atomic electrons into continuum (shake-off process) and a decay of a shake-up satellite into continuum [1]. The Green's function theory of lineshapes of satellites in photoelectron spectra, accounting for these processes, was developed in references [6,7]. The theoretical prediction [6,7] of the Fano-type [8] asymmetry with raised high binding energy side of all broad photoelectron satellites, based on calculations for Ne, was also supported experimentally for Ar [3]. The excited two-hole-one-particle (satellite) states are decaying into underlying continuum, giving rise to valence Auger lines with very small kinetic energies [9,10] (low-energy Auger spectra). Unfortunately there are no special characterization of the shapes of valence Auger lines [10], but the pictures of reference [10] clearly show a pronounced Fano-type asymmetry of both directions. Most of theoretical works [11–14] were aimed to the calculations of Lorentzian linewidths of satellite states, but no theoretical estimations for the shapes of the Auger lines originating from the excited atomic states exist.

According to the Green's function theory for the Auger spectra [15] the widths of the Auger lines, originating from main (Lorentzian) photoelectron lines, equal to the width of the photoelectron line and the intensity of each Auger line is proportional to its partial width (contribution to the photoelectron linewidth). On the other hand low-energy Auger spectra [10] show a strong Fano-type asymmetry of both directions of asymmetry. Since these Auger lines originate from the states of one direction of asymmetry (or symmetrical states), it follows that the theory of Auger lineshapes should be generalized to describe the decay of excited atomic states. This is main aim of the present work.

In the present work the approach of reference [7] is further developed in order to obtain the formulae for the calculation of low-energy Auger lineshapes. The lineshapes for the Auger decay into underlying continua of the satellite states $[2s2p](^{1,3}P)3s(^2P)$, $[2s2p](^1P)4s(^2P)$ and $[3s3p](^3P)4s(^2P)$ in valence p-photoelectron spectra of Ne and Ar atoms are calculated. (Hole states are indicated by square brackets throughout). The calculations show that in some cases the widths and the shapes of Auger lines are approximately equal to that of the primary photoelectron satellite line, but in other cases a significant difference occurs. Numerical calculations show a new appearance of many-electron correlations: the Auger decay lines of satellites in photoelectron spectra can be narrower and their asymmetry can be different than those of the primary satellite photoelectron line. Theoretical results are in reasonable agreement with low-energy Auger spectra [10].

[a] e-mail: vgyar@ionchran.rinet.ru

2 Theory

If the photon energy is far above the threshold, the total energy distribution of the k-hole state is given by the spectral function [6,7,16,17]:

$$A(E) = \frac{1}{\pi} \frac{\Im\Sigma(E)}{(E - \varepsilon_k - \Re\Sigma(E))^2 + \Im\Sigma(E)^2} \quad (1)$$

where $\Re\Sigma$ and $\Im\Sigma$ are real and imaginary parts of the self-energy, ε_k is the one-electron energy of the hole under consideration and E is the energy parameter.

All important channels of excitation and decay should be included in real and imaginary parts of the self-energy. Let us consider the excitation from the initial hole $[k]$ into a double-hole-one particle discrete satellite state $[il]r$ in the presence of several underlying continuum states $[ij_\nu]c_\nu$. It was shown [1,7] that in this case the lineshape is influenced by both direct transitions into continuum $[k] \to [ij_\nu]c_\nu$ and by two-step process $[k] \to [il]r \to [ij_\nu]c_\nu$. In order to take into account both these processes one should consider a limited set of diagrams up to the fourth order of perturbation theory [7]. It should be mentioned that the theory of lineshapes in photoelectron spectra in the presence of several channels of broadening was developed in reference [18], but only the case of constant broadening parameters was considered there. We will see below, that the main features of asymmetrical broadening of satellite states and of their Auger decay channels are due to a very strong variation of hole state energy parameters ($\Re\Sigma$ and $\Im\Sigma$).

Since the total number of fourth order diagrams is very high we consider briefly the physical background of our choice of the diagrams responsible for the linewidths. The diagrams should describe two main channels of broadening [1] and, since formula (1) defines the spectral density, the $\Im\Sigma$ should be positively defined on all energy axes. We consider below the imaginary parts of higher order diagrams, but real parts of these diagram are also taken into account.

The second order diagrams represent the broadening of the satellite due to the direct transitions from one-hole states to the continuum $[k] \to [ij_\nu]c_\nu$ (shake-off process). The term of the imaginary part of the self-energy corresponding to this process is given by the following formula [16,17]:

$$\Im\Sigma_2(E) = \sum_\nu \pi U^2_{kj_\nu ic_\nu}(\varepsilon_{c_\nu}) \delta(E - \varepsilon_i - \varepsilon_{j_\nu} + \varepsilon_{c_\nu}) \quad (2)$$

where $U_{kj_\nu ic_\nu}$ is the Coulomb matrix element of Auger decay of the initial one-hole state $[k]$ into two-hole-one-particle state $[ij_\nu]c_\nu$ [19].

The broadening of the line due to the two-step process $[k] \to [il]r \to [ij_\nu]c_\nu$ is described by the fourth order diagram of perturbation theory [7] and the corresponding term of the imaginary part of the self-energy is written as:

$$\Im\Sigma_4(E) = \sum_\nu \pi U^2_{klir} U^2_{lrj_\nu c_\nu}(\varepsilon_{c_\nu}) \times \delta(E - \varepsilon_i - \varepsilon_{j_\nu} + \varepsilon_{c_\nu})/\Delta^2. \quad (3)$$

The matrix elements $U^2_{lrj_\nu c_\nu}$ of interaction between two-hole-one-particle states are calculated making use of the graphical technique [20]. The sign of the corresponding Feynman diagram [21] is also included in this matrix element. The value Δ in formula (3) is defined as:

$$\Delta = E - \varepsilon_i - \varepsilon_l + \varepsilon_r. \quad (4)$$

It is the shift of the energy parameter with respect to the one-electron Hartree-Fock position of the satellite. Since in the satellite energy region this value is small, $\Im\Sigma_4$ in formula (3) varies sharply. In order to envisage the physical significance of this term we consider the main (second order) term of the real part of the self-energy [16,17]:

$$\Re\Sigma_2(E) = \sum_r \frac{U^2_{klir}}{E - \varepsilon_i - \varepsilon_l + \varepsilon_r} + \int_0^\infty \frac{U^2_{klir} d\varepsilon_r}{E - \varepsilon_i - \varepsilon_l + \varepsilon_r}. \quad (5)$$

The position of the line is given by the solution of the Dyson equation [16,17]:

$$E^*_r = \varepsilon_k + \Re\Sigma(E^*_r). \quad (6)$$

The intensity of the line is proportional to its spectroscopic factor:

$$f = \frac{1}{1 - \dfrac{\partial\Re\Sigma(E)}{\partial E}} \quad (7)$$

where the derivative is taken at point E^*_r.

The Lorentzian linewidth is given by the following formula [16]:

$$\Gamma = 2f\Im\Sigma(E^*_r). \quad (8)$$

Inserting (2) into (8) we obtain the line broadening due to direct excitation into the shake-off continuum:

$$\Gamma_0 = 2\pi f \sum_\nu U^2_{kj_\nu ic_\nu}(\varepsilon_{c_\nu}) \delta(E^*_r - \varepsilon_i - \varepsilon_{j_\nu} + \varepsilon_{c_\nu}). \quad (9)$$

In the vicinity of the satellite under consideration we retain only one term in the sum in right hand side of (5) corresponding to it and neglect the integral. For small satellites we can also neglect unity in the denominator of (7) and obtain:

$$f \approx \frac{\Delta^{*2}}{U^2_{klir}} \quad (10)$$

where $\Delta^* = E^*_r - \varepsilon_i - \varepsilon_l + \varepsilon_r$ is the energy shift of the top of the line with respect to the one-electron value.

Making use of equations (3, 8, 10) we obtain the line broadening due to the direct interaction of the satellite state with the continuum:

$$\Gamma_r = 2\pi \sum_\nu U^2_{lrj_\nu c_\nu}(\varepsilon_{c_\nu}) \delta(E - \varepsilon_i - \varepsilon_{j_\nu} + \varepsilon_{c_\nu}). \quad (11)$$

The width Γ_r was calculated in references [11–13]. Since in the satellite series under consideration spectroscopic factors are small (about 0.01), the value of Γ_0 is smaller than Γ_r [7].

The third order term of the self-energy decomposition represents the interference term between the two above mentioned channels which contribute to the broadening:

$$\Im\Sigma_3 = \sum_\nu 2\pi U_{klir} U_{lrj_\nu c_\nu}(\varepsilon_{c_\nu}) U_{kj_\nu ic_\nu}(\varepsilon_{c_\nu}) \times \delta(E - \varepsilon_i - \varepsilon_{j_\nu} + \varepsilon_{c_\nu})/\Delta. \quad (12)$$

The strongly non-Lorentzian lineshapes of broad satellites follows directly from formulae (1, 5), since when the energy parameter E approaches the one-electron energy of the satellite $\varepsilon_i + \varepsilon_l - \varepsilon_r$, the $\Re\Sigma$ in formula (5) approaches infinity, and the spectral density (1) approaches zero. Hence it follows that the line is Lorentzian only if:

$$\Delta^* \gg \Gamma. \quad (13)$$

For the alternative case, *i.e.* when:

$$\Delta^* \approx \Gamma, \quad (14)$$

one side of the line is effectively depressed and its shape is asymmetrical. Since all the shake-up satellites are shifted to the higher binding energy side from the Hartree-Fock position, the low-binding energy side of all broad shake-up satellites is effectively depressed [7]. This theoretical assertion was confirmed experimentally [3]. Hence it follows that the lineshape of the satellite is asymmetrical in the case when the direct interactions with the continuum are not taken into account and the direction of this asymmetry is fixed. On the other hand there is no preferential direction for the asymmetry associated with autoionization resonances [8]. This main difference between the photoelectron satellites and autoionization resonances follows from the different origins of these states. The origin of the photoelectron satellites is due to electron-electron correlations and corresponding terms appear in the second order of perturbation theory. On the other hand the autoionized states appear due to the direct interaction between atomic electrons and photons.

The Green's function technique makes it possible to obtain also the formulae for the spectral function of Auger transitions. For each channel of broadening the imaginary part of the self-energy may be written as:

$$\Im\Sigma^\nu(E) = \Im\Sigma_2^\nu(E) + \Im\Sigma_3^\nu(E) + \Im\Sigma_4^\nu(E) \quad (15)$$

where terms in right hand side of (15) are defined by formulae (2, 12, 3). It follows from these formulae that $\Im\Sigma^\nu(E)$ is a positively defined function at any point of the energy axis, where this function exists. This assertion reinforces our choice of higher order diagrams in the decomposition of the imaginary part of the self-energy.

In the case of Ne and Ar the probabilities of the radiative transitions are much less than the probabilities of Auger transitions [11,12]. In this case one can neglect the terms in the imaginary part of the self-energy connected with radiative transitions [15]. Thus the imaginary part of the self-energy may be expressed as the sum over all channels of the Auger decay:

$$\Im\Sigma(E) = \sum_\nu \Im\Sigma^\nu(E). \quad (16)$$

Making use of (16) we can write instead of (1):

$$A(E) = \sum_\nu A^\nu(E) = \sum_\nu \frac{1}{\pi} \frac{\Im\Sigma^\nu(E)}{(E - \varepsilon_k - \Re\Sigma(E))^2 + \Im\Sigma(E)^2}. \quad (17)$$

Since the δ-functions in terms of second, third and fourth order are the same for the same ν-values, formula (17) makes it possible to distribute the main line intensity into parts corresponding to subsequent Auger decay into different ν-channels. It should be pointed out that a formula very similar to (17) was obtained in reference [15], but only the case of constant $\Im\Sigma$ was considered there. It follows from formula (17) that in this case the widths of all Auger lines are equal to the width of the primary photoelectron line and that the distribution of the photoelectron line spectral density between Auger transitions is constant. This is usually valid for main photoelectron lines. In the case of photoelectron satellites the values of $\Im\Sigma^\nu$ may vary very significantly. Hence, it follows that the distribution of the photoelectron line spectral density between Auger transition is a strongly energy dependent function. This may result in interesting effects. In order to give further insight into these effects, numerical calculation for Ne and Ar are carried out in the next section.

3 Numerical calculations

In the present work we consider four satellites: three satellites associated with $[2s2p](^{1,3}P)3s(^2P)$ and $[2s2p](^1P)4s(^2P)$ configurations in the $2p$-photoelectron spectrum of Ne (lines 60, 67 and 69 [3]) and a satellite associated with the $[3s3p](^3P)4s(^2P)$ configuration in $3p$-photoelectron spectrum of Ar (line 68 [3]). These lines are broadened due to inner-valence Auger transitions into the underlying continua $[np^2](^3P,^1D,^1S)\varepsilon p(^2P)$ [11,12]. Due to its higher binding energy the satellite $[2s2p](^1P)4s(^2P)$, may deexcite *via* a valence-multiplet transition into the $[2s2p](^3P)$ continuum.

The computer code Atom [22] was used to calculate the wavefunctions in the Hartree-Fock approximation. There are two different methods for the calculation of the wavefunctions [6]. In the relaxed approximation the two-hole configuration is calculated self-consistently and the excited-state wavefunctions are calculated in this field. In the frozen approximation the atomic ground state wavefunctions are used for the calculation of the excited states in a field of two holes. The frozen approximation is more appropriate for the calculation of the intensities of the valence-shell satellites [6,23]. The relaxed approximation

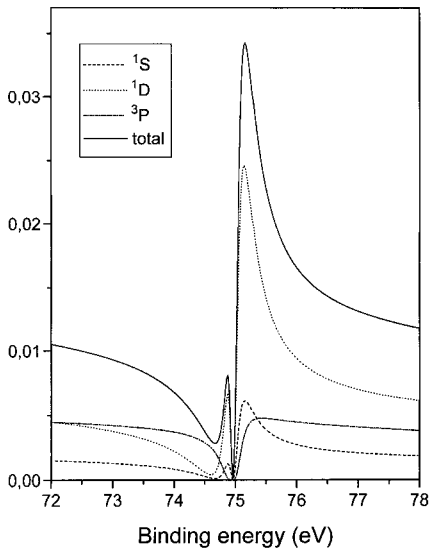

Fig. 1. Spectral functions (arbitrary units) of valence Auger decay of $[2s2p]({}^3P)3s({}^2P)$ satellite (line 60) in Ne; dashed line: decay into $[2p^2]({}^1S)$ final state, dotted line: decay into $[2p^2]$-$({}^1D)$ final state, dashed-dotted line: decay into $[2p^2]({}^3P)$ final state, solid line: total (spectral function of the $[2s2p]({}^3P)3s$-$({}^2P)$ satellite).

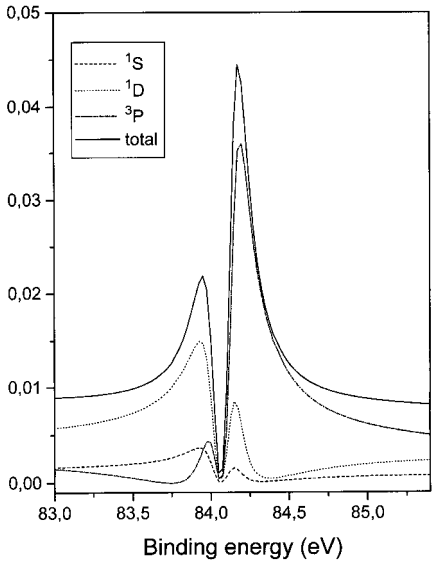

Fig. 2. Spectral functions (arbitrary units) of valence Auger decay of $[2s2p]({}^1P)3s({}^2P)$ satellite (line 67) in Ne; dashed line: decay into $[2p^2]({}^1S)$ final state, dotted line: decay into $[2p^2]$-$({}^1D)$ final state, dashed-dotted line: decay into $[2p^2]({}^3P)$ final state, solid line: total (spectral function of the $[2s2p]({}^1P)3s$-$({}^2P)$ satellite).

is more suitable for the calculation of final state configuration interaction effects. The interaction of the valence satellite states with the underlying continuum which defines the value of Γ_r (see formula (11)) is the appearance of final state configuration interaction. The widths Γ_r of the satellites $[2s2p]({}^1P)3s({}^2P)$ and $[2s2p]({}^3P)3s({}^2P)$ calculated in the relaxed approximation [11] equal to 0.238 eV and 0.334 eV respectively and are in a good agreement with experimental [4] values 0.206 ± 0.041 eV and 0.42 ± 0.09 eV. The frozen approximation [7] seems to overestimate the experimental widths [4]. Since the present work is aimed to the calculations of the lineshapes the relaxed approximation is used throughout.

The spectral functions of the satellites in question together with the spectral functions of valence Auger transitions are shown in Figures 1–4. The binding energy scale was used both for the photoelectron and the Auger spectral functions. The kinetic energy distribution of the Auger electrons can be easily obtained making use of the known experimental satellite binding energies [3] and double-ionization thresholds [10].

The spectral functions of the satellite $[2s2p]({}^3P)3s$-$({}^2P)$ (line 60) in the photoelectron spectrum of Ne and that of the Auger transitions into $[2p^2]({}^3P, {}^1D, {}^1S)\varepsilon p({}^2P)$ continua are shown in Figure 1. When fitting the theoretical curve with a Fano profile we obtained the width 0.37 eV, which is in a good agreement with the experimental value 0.42 [4].

In the resonant part of the spectrum the intensity of the Auger transition into the ^1D continuum is the most intense one. Due to interference effects between two transition paths to the ^3P continuum, its intensity is suppressed at the top of the line. When coming from the resonant part of the peak to a non-resonant part, the intensities of transitions into ^1D and ^3P continua become approximately equal. The spectral distribution of Auger electrons in the ^1S continuum is similar to that in the ^1D continuum, but due to the smaller matrix elements it is significantly smaller in magnitude.

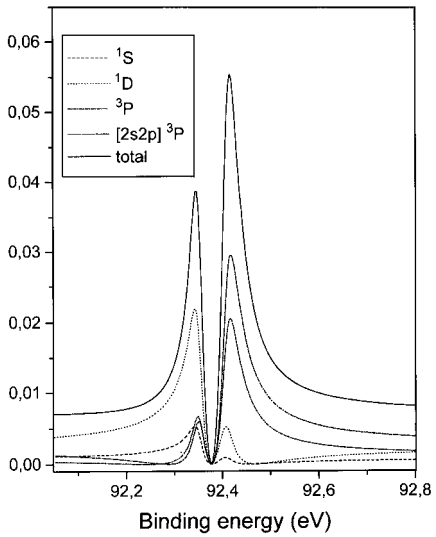

Fig. 3. Spectral functions (arbitrary units) of valence Auger decay of $[2s2p]({}^1P)4s({}^2P)$ satellite (line 69) in Ne; dashed line: decay into $[2p^2]({}^1S)$ final state, dotted line: decay into $[2p^2]$-$({}^1D)$ final state, dashed-dotted line: decay into $[2p^2]({}^3P)$ final state, dashed-double-dotted line: decay into $[2s2p]({}^3P)$ final state, solid line: total (spectral function of the $[2s2p]({}^1P)4s$-$({}^2P)$ satellite).

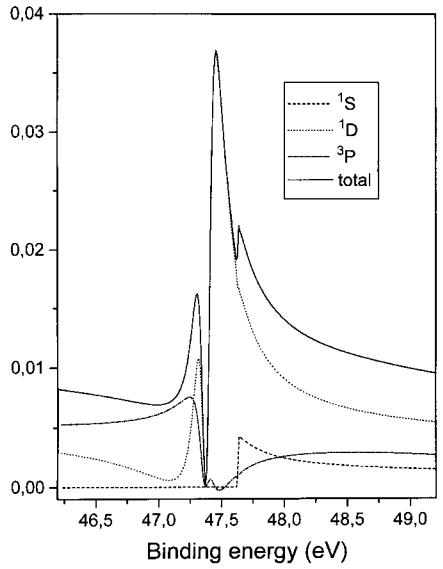

Fig. 4. Spectral functions (arbitrary units) of valence Auger decay of $[3s3p]({}^3P)4s({}^2P)$ satellite (line 68) in Ar; dashed line: decay into $[3p^2]({}^1S)$ final state, dotted line: decay into $[3p^2]$-$({}^1D)$ final state, dashed-dotted line: decay into $[3p^2]({}^3P)$ final state, solid line: total (spectral function of the $[3s3p]({}^3P)4s$-$({}^2P)$ satellite).

Figure 2 shows the same for the satellite $[2s2p]({}^1P)$-$3s({}^2P)$ (line 67 [3]) in photoelectron spectrum of Ne. It is seen from Figure 2, that at the top of the photoelectron line the main channel of Auger decay is into the $[2p^2]({}^3P)$ continuum. There is a strong interference between two channels causing broadening for the transitions into the $[2p^2]({}^1D)$ and $[2p^2]({}^1S)$ continua in the energy region near the top of the satellite profile, and the intensities of these transitions are shifted to lower binding energies.

Theoretical satellite lineshape prediction reveals a trough between spectral densities corresponding to transitions into the ${}^3P$ and ${}^1D$ (${}^1S$) continua. In the experimental spectrum [3] this trough is smeared by instrumental broadening (FWHM = 0.17 eV [3]) and by spin-orbit splitting (0.1 eV [5]). The experimental spectrum [3] show complex structure at the low binding energy side of this satellite. But this structure is also due to overlap with the satellite $[2s2p]({}^3P)5p({}^2S)$ [1–4].

Figure 3 shows the spectral function for the satellite $[2s2p]({}^1P)4s({}^2P)$ (line 69 [3]) in photoelectron spectrum of Ne. The distribution of the satellite line intensity between different channels of $[2p^2]$ continua is approximately the same as in a previous case. The trough between peaks is very narrow and it may not be seen in the photoelectron spectrum. Due to the higher binding energy of this satellite state a new channel of decay into $[2s2p]({}^3P)$ continuum opens. The Auger spectral density of this transition is in the same binding energy region as that for the $[2p^2]({}^3P)$ continuum.

The satellite 68 in photoelectron spectrum of Ar was assigned [3] as the state $[3s3p]({}^3P)4s({}^2P)$. This satellite is very similar to the line $[2s2p]({}^3P)3s({}^2P)$ in photoelectron spectrum of Ne. It is very broad and reveals a pronounced Fano-like profile. Since the threshold of ${}^1S$ continuum is near the top of this line, its structure is complex [3]. Theoretical spectral function prediction for this satellite (see Fig. 4) correctly reproduces its asymmetrical shape. The main channel of decay is into the ${}^1D$ continuum. The prediction is that the decay into the ${}^3P$ continuum is rather small. The channel of decay into ${}^1S$ continuum opens after the top of the line and there is no Auger line in this continuum.

4 Discussion

Our calculations reveal two essential features of the lineshapes as a result of the Auger decay of the photoelectron satellite states:

1. when decaying into the continuum the symmetrical satellite states and the satellite states of one direction of asymmetry result in Auger lines with sharp Fano-type profiles in both directions of asymmetry;
2. in some cases the Auger decay lines may be narrower than the parent photoelectron satellite lines.

These unusual features are due to very strong electron-electron correlation involving the continuum states.

Experimental photoelectron spectra show asymmetry on the high binding energy (low kinetic energy) side of all the broad satellites [3]. Using energy conservation principles one can expect the asymmetry of associated Auger lines to be on the high kinetic energy side. This direction of asymmetry is considered to be normal. Some of the experimentally observed valence Auger transitions are assigned in reference [10] and therefore we can carry a comparison between theory and experiment.

In accordance with our theory (see Fig. 1) the direction of asymmetry of Auger decay line of the Ne satellite $[2s2p]({}^3P)3s({}^2P)$ into the $[2p^2]({}^1D)$ continuum (Auger line with kinetic energy 9.4 eV) is normal [10]. The threshold for the $[2p^2]({}^1D)$ continuum is 65.73 eV [10]. We can also estimate the threshold of the continuum $[2p^2]({}^3P)$ from Figure 7 of reference [10] as 62.5 eV. The energy difference between the two continuum thresholds is therefore 3.2 eV. When shifting from the point $E_{kin} = 9.4$ eV to the point 12.6 eV no experimental peak is observed [10]. The theoretical explanation is that the intensity for the transition to $[2p^2]({}^3P)$ is very small, and the corresponding Auger lines are not seen. Thus for the satellite 60 experimental low-energy Auger spectra unambiguously confirm all the theoretical results.

It is seen from Figure 2 that the theoretical direction of asymmetry of Auger decay of the satellite $[2s2p]({}^1P)$-$3s({}^2P)$ into ${}^1D$ continuum is reversed to the lower binding energy side. The experimental results [10] also show the reversed direction of asymmetry for the Auger decay line of the state $[2s2p]({}^1P)3s({}^2P)$ into the ${}^1D$ continuum. (Auger line with kinetic energy 19.2 eV). The contribution to the Auger decay of the satellite $[2s2p]({}^3P)5p({}^2S)$ should be also taken into account. The intensity of the satellite $[2s2p]({}^3P)5p({}^2S)$ is approximately 20 times lower than that of the state $[2s2p]({}^1P)3s({}^2P)$ [3] with almost all

of its intensity transferred to the ^1D Auger channel. The theoretical ratio of the intensities of Auger transitions may be estimated from Figure 2 as $I(^1D)$:$I(^3P) = 1$:2.4 Thus the contribution of the satellite $[2s2p](^3P)5p(^2S)$ to the Auger line under consideration is approximately 6 times less than that of the satellite $[2s2p](^1P)3s(^2P)$. A very strong trough on the high kinetic energy side is a characteristic feature of this Auger line (see Fig. 4 in Ref. [10]). This experimental result is in excellent agreement with the theory.

The next Auger line ($E_{kin} = 22.4$ eV) was assigned [10] to be the Auger transition $[2s2p](^1P)3p(^2S) \rightarrow [2p^2](^1D)$. However, the energy difference between this line and the previous line is exactly 3.2 eV, *i.e.* difference between the ^1D and ^3P thresholds. Hence, it follows that this line may be also assigned as the Auger transition $[2s2p]$-$(^1P)3s(^2P) \rightarrow [2p^2](^3P)$. The relative intensities of these transitions may be estimated as follows. The intensity of satellite $[2s2p](^1P)3s(^2P)$ is 36% of the intensity of the satellite $[2s2p](^1P)3p(^2S)$ [3] but only less a 1% of its intensity is transferred to the ^1D continuum channel [11]. Thus the Auger line a with kinetic energy of 22.4 eV is mainly due to the transition $[2s2p](^1P)3s(^2P) \rightarrow [2p^2]$-$(^3P)$. No direction of asymmetry for this line is observed in the experimental spectrum [10].

The Auger line with $E_{kin} = 26.1$ eV was assigned as $[2s2p](^1P)4s(^2P) \rightarrow [2p^2](^1D)$. In agreement with the theory this line shows a reversed asymmetry.

In the case of Ar the structure of the valence Auger spectrum is more complex [10]. The interpretation is limited and we are not able to perform complete comparison of the theory with the experiment. The agreement of the theoretical lineshape of photoelectron satellite $[3s3p](^3P)4s(^2P)$ with the shape of the experimental line 68 [3] is excellent.

5 Conclusion

The theory of lineshapes of Auger transitions from the multiple vacancy satellite states accompanying photoionization is developed. It is shown that two different cases for lineshape profiles are possible. In the first case (similar to the Auger decay of inner holes [15]) the widths and the shapes of the valence Auger lines are the same as for the primary photoelectron line (examples are the decay of the satellite states $[nsnp](^3P)(n+1)s(^2P)$ in Ne and Ar into the ^1D continuum). But in the second case some Auger channels can disappear (examples are the decay of the states $[nsnp](^3P)(n+1)s(4s)(^2P)$ in Ne and Ar into the ^3P continuum) or their widths can be smaller and the directions of asymmetry can be reversed with respect to primary photoelectron lines (examples decay of the states $[2s2p](^1P)ns(^2P)$ $(n = 3, 4)$ in Ne into the ^1D continuum). Most of the theoretical results are in reasonable agreement with the known experimental photoelectron [3] and low-energy Auger [10] spectra. A theoretical prediction is that the profile on the high binding energy side of the photoelectron satellite $[2s2p](^1P)3s(^2P)$ results from deexcitation into the ^3P continuum while the low binding energy side of the profile results from deexcitation into the ^1D continuum.

We thank M.Ya. Amusia and L.V. Chernysheva for their computer code Atom and useful discussions. The authors are grateful to the School of Chemistry, University of Melbourne for the financial support. The financial support of Russian Basic Research Foundation (grant 96-15-97388) is greatly acknowledged by V.G.Y.

References

1. S. Svensson, B. Ericsson, N. Martensson, G. Wendin, U. Gelius, J. Electron Spectrosc. Relat. Phenom. **47**, 327 (1988).
2. U. Becker, J. Electron Spectrosc. Relat. Phenom. **75**, 23 (1995).
3. A. Kikas, S.J. Osborne, A. Ausmees, S. Svensson, O.-P. Sairanen, S. Aksela, J. Electron Spectrosc. Relat. Phenom. **77**, 241 (1996).
4. M. Pahler, C.D. Caldwell, S.J. Schaphorst, M.O. Krause, J. Phys. B. **26**, 1617 (1993).
5. M.O. Krause, S.B. Whitfield, C.D. Caldwell, J.-Z. Wu, P. van der Meulen, C.A. de Lange, R.W.C. Hansen, J. Electron Spectrosc. Relat. Phenom. **58**, 79 (1992).
6. V.G. Yarzhemsky, G.B. Armen, F.P. Larkins, J. Phys. B. **26**, 2785 (1993)
7. V.G. Yarzhemsky, A.S. Kheifets, G.B. Armen, F.P. Larkins, J. Phys. B. **28**, 2105 (1995).
8. U. Fano, Phys. Rev. **124**, 1866 (1961).
9. U. Becker, R. Wehlitz, O. Hemmers, B. Langer, A. Menzel, Phys. Rev. Lett. **63**, 1054 (1989).
10. U. Becker, R. Wehlitz, J. Electron Spectrosc. Relat. Phenom. **67**, 341 (1994).
11. G.B. Armen, F.P. Larkins, J. Phys. B. **24**, 741 (1991).
12. G.B. Armen, F.P. Larkins, J. Phys. B. **25**, 931 (1992).
13. M.Ya. Amusia, I.S. Lee, V.A. Kilin, J. Phys. B. **25**, 657 (1992).
14. C. Sinanis, G. Aspromallis, C.A. Nicolaides, J. Phys. B. **28**, L423 (1995).
15. M. Ohno, G. Wendin, J. Phys. B. **8**, 1305 (1979).
16. G. Wendin, *Structure, Bonding*, Vol. 45 (Heidelberg, Springer, 1981), p. 1.
17. M.Ya. Amusia, A.S. Kheifets, Sov. Phys-JETP **59**, 710 (1984).
18. G. Wendin, Comm. Atom. Molec. Phys. **17**, 115 (1986).
19. D.L. Walters, C.P. Bhalla, Phys. Rev. A. **3**, 1919 (1971)
20. I. Lindgren, J. Morrison, *Atomic many-body theory* (Springer, Berlin, 1982).
21. B.R. Judd, *Second quantization and atomic spectroscopy* (John Hopkins, Baltimore, 1967).
22. M.Ya. Amusia, L.V. Chernysheva, *Computation in Atomic Physics* (IOP Publishing Ltd., Bristol, 1997).
23. A.S. Kheifets, J. Phys. B. **28**, 3791 (1995).